PROCEEDINGS, 49th Workshop on Geothermal Reservoir Engineering
Stanford University, Stanford, California, February 12-14, 2024
SGP-TR-227

Development of an Integrated Reservoir and Production System Modelling (IPSM) Workflow for simulating CO_2-Plume Geothermal (CPG) Systems at the Aquistore CCS Site

Kevin P. Hau[1], Maren Brehme[1], Alireza Rangriz Shokri[2], Reza Malakooti[3], Erik Nickel[4], Rick J. Chalaturnyk[2], Martin O. Saar[1,5]

[1]Geothermal Energy & Geofluids Group, Institute of Geophysics, Department of Earth Sciences, ETH Zurich, Zurich, Switzerland, (hauk @ ethz.ch)

[2]Department of Civil and Environmental Engineering, University of Alberta, Edmonton, AB, Canada

[3]Computer Modelling Group Ltd., Oxford, UK

[4]Petroleum Technology Research Centre, Regina, SK, Canada

[5]Department of Earth and Environmental Sciences, University of Minnesota, Minneapolis, MN, USA

Keywords: Keywords: Geothermal Energy, CCUS, Decarbonisation, Reservoir Engineering, Energy Transition

ABSTRACT

A strong reduction in global carbon dioxide (CO_2) emissions is necessary to achieve the climate targets set out in the Paris Agreement. Decarbonisation of the energy sector, for example, requires baseload renewable energy sources, while decarbonisation of the cement and other heavy industries requires active capture and permanent (geologic) sequestration of CO_2 (e.g. carbon, capture, and storage (CCS)). So far, economic constraints prevent the commercial-scale deployment of the CCS technology. Geothermal energy, as one of the renewable energy sources, can provide significant baseload energy supply but is restricted to regions with high (a) geothermal gradients and (b) rock transmissivities. Often, one of these is not given, limiting economic geothermal energy extraction.

The usage of supercritical CO_2 as a geothermal working fluid by injecting it and circulating it in a closed system from the reservoir to the Earth's surface to extract the geothermal energy can open possibilities in regions that are otherwise economically disadvantageous for geothermal energy use. Previous studies have shown that the theoretical efficiency of a geothermal system can be doubled to tripled, compared to conventional geothermal systems, due to the significantly lower kinematic viscosity of supercritical CO_2, compared to H_2O. This concept is commonly known as CO_2-Plume Geothermal (CPG). It uses (eventually) permanently sequestered CO_2 from a CCS site to a) improve the business case of CCS systems by generating geothermal power (thermal and/or electric) and b) reduce the reservoir temperature and pressure, which in turn increases the overall CO_2 storage capacity and safety.

In our numerical feasibility study, we investigate the suitability of the active, commercial-scale, research-oriented Aquistore CCS site in Canada for a CO_2-circulation demonstration test. We apply a pioneering workflow, combining (1) a field history-matched, heterogeneous reservoir model with (2) a full-physics fluid flow simulator, (3) a wellbore and (4) a simplified surface facility model (representing surface energy extraction and CO_2 reinjection) in an integrated manner.

1. INTRODUCTION

The consequences of accumulating greenhouse gas concentrations in the atmosphere in the currently unfolding climate crisis, are omnipresent and becoming more extreme year by year (IPCC, 2023). Global greenhouse gas emissions (e.g. CO_2) must be drastically reduced to reach the climate goals set by the Paris Agreement (i.e. limiting the average global temperature to 1.5°C). The global energy system is transitioning with a peak in fossil fuel energy consumption insight before 2030 (IEA, 2023). Based on today's policy settings, the International Energy Agency expects a decline in the share of fossil fuels in the global energy supply from currently around 80% to around 73% by 2030. Moreover, global energy-related greenhouse gas emissions are expected to peak by 2025 (IEA, 2023). Nevertheless, transitioning the energy system towards renewable and carbon-neutral baseload-capable energy sources and the permanent isolation of CO_2 from the atmosphere are two major challenges in particular for this decade and likely for several decades to come.

The CO_2 Capture and Sequestration (CCS) technology can be used to capture CO_2 at point sources or remove directly from the atmosphere and store it permanently in geological formations (IPCC, 2023). However, the CCS industry is still in its infancy. Improving the economics of CCS, for example by reducing costs or increasing CO_2 sequestration capacities and efficiencies will benefit CCS development. At the same time, baseload-capable geothermal energy has enormous potential for the global energy transition, even though its development depends strongly on sufficiently high temperatures and permeabilities in the relatively shallow (2–5 km) subsurface. Referred to as CO_2-Plume Geothermal (CPG) systems (e.g. Randolph & Saar, 2011), the use of geologically stored supercritical CO_2 as a geothermal energy extraction fluid may open so far economically unattractive geological regions for cost-competitive geothermal energy extraction and even electricity generation, such as reservoirs at 2–3 km depths within sedimentary basins that exhibit standard continental-crust geothermal gradients of ~30°C/km and/or relatively low permeabilities below ~10^{-13} m^2 (Adams et al., 2015). The improved performance of supercritical CO_2, compared to water, results from the significantly higher mobility ($\frac{\rho_{fluid}}{\mu_{fluid}}$) of supercritical CO_2, compared to water, at reservoir depths of 2–5 km, resulting in an equivalently larger massflow rate, $\dot{m}_{fluid}$ [kg/sec]:

$$\dot{m}_{fluid} = \frac{k_{abs} k_{rel}\ \rho_{fluid}}{\mu_{fluid} L} A\ \Delta P = \frac{\rho_{fluid}}{\mu_{fluid}} * \frac{k_{abs} k_{rel}}{L} A\ \Delta P \quad (1)$$

where k_{abs}, and k_{rel} are the absolute [m^2] and relative permeability [-], receptively, μ_{fluid} and ρ_{fluid} represent the fluid's dynamic viscosity [mPa sec] and density [kg/m^3], respectively, L is the distance [m], A is the cross-sectional area [m^2] between the wells, and ΔP is the pressure drop [Pa] along L. Table 1 lists the thermophysical properties of supercritical CO_2, pure water, and a hypersaline brine with a salinity of 300'000 ppm (similar to the Aquistore brine). From Equation (1) and Table 1, one can see, how the fluid-specific properties, first term, affect the total massflow rate. For supercritical CO_2, this factor reaches >12'200, while water and brine only reach values of ~3'750. Nevertheless, Equation (1) yields only a one-dimensional approximation for massflow rates within the reservoir. It is important to acknowledge that the thermophysical properties of CO_2 are highly dependent on both temperature and pressure. Consequently, even slight variations in these parameters may lead to significant deviations in the massflow rate.

Table 1: Thermophysical properties of supercritical CO_2 (sCO_2), H_2O and a 300'000 ppm brine at reservoir conditions with T = 113°C and P = 35 MPa (Bell et al., 2014; Ezekiel et al., 2022).

Parameter		CO_2	H_2O	Brine
μ_{fluid}	[mPa sec]	0.053	0.256	0.323
ρ_{fluid}	[kg/m^3]	647.76	963.9	1'205.6
$\frac{\rho_{fluid}}{\mu_{fluid}}$	[sec/m^2]	~ 12'220	~ 3'765	~ 3'732

CO_2 plume geothermal system have been modelled numerically in earlier work (e.g. Adams et al., 2015; Ezekiel et al., 2022). However, all these studies employ conceptual reservoir models and use multiple software tools to model reservoir, wellbore, and surface facilities separately. In our study, we present an integrated reservoir and production system modelling (IPSM) workflow, capable of modelling a CPG system in its entirety. The newly developed workflow is the applied to the field-data-constrained geological model of the Canadian Aquistore CCS site, where CO_2 has been injected since 2015 (PTRC, 2015). The location of the site is within the intracratonic sedimentary basin known as the Williston Basin, covering more than 250,000 km^2 in North America. The basin underlays parts of Saskatchewan, Manitoba, and Alberta in Canada as well as Montana and North and South Dakota in the United States (Guyant et al., 2015). Sedimentary basin deposits typically exhibit cycles of transgressive and regressive periods (Catuneanu, 2022). Hence, the sedimentary layers usually consist of different lithologies, such as sandstones, red beds, carbonates, shales, and other evaporites. Often variations in lithology correspond with a change in the rock's petrophysical properties, such as permeability and thermal conductivity. Sedimentary basins, like the Williston Basin, are widespread globally (White et al., 2016) and provide a large potential for a) CO_2 storage and b) geothermal energy extraction. The Aquistore CCS project exemplifies CO_2 sequestration in the Williston Basin, while DEEP Earth Energy Production Corp. envisions the sustained development of 200 MW of geothermal energy within the same basin .

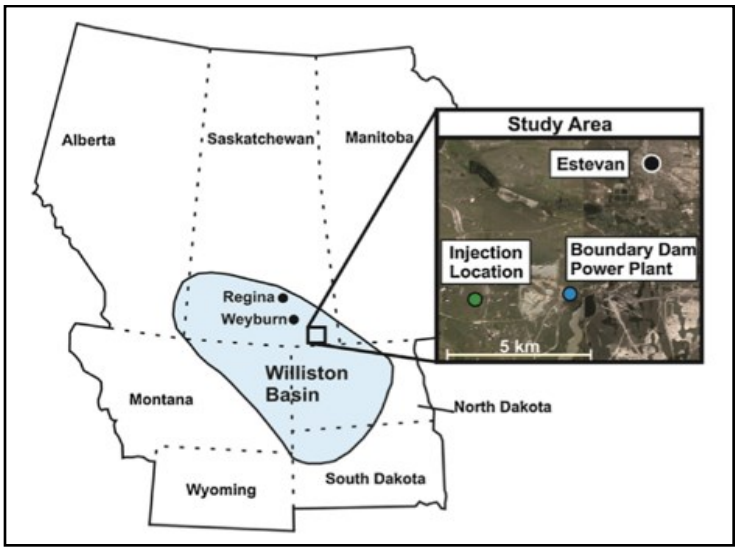

Figure 1: Schematic map showing the lateral extent of the Williston Basin and a superimposed satellite image of the Aquistore CCS site with the CO_2 injection well, the Boundary Dam power plant, where the CO_2 is captured, and the city of Estevan indicated (Guyant et al., 2015).

At Aquistore, the Cambrian Deadwood and Winnipeg formations serve as the reservoir units, while the Icebox formation functions as the caprock, respectively. The Deadwood formation is a thick and wide-spread mixed siliciclastic unit that marks the beginning of the sediment filling of the Williston Basin on top of the Precambrian surface (Kreis et al., 2004). At Aquistore, the Deadwood formation is a 147 m thick unit, characterised by interbedded sandstones, shales, and siltstones. The Winnipeg formation consists of the lowermost Black Island unit. It is overlain by the Icebox unit, consisting of a 30 m thick shale that serves as the main sealing unit, preventing vertical CO_2 migration.

CO_2 is captured at the Boundary Dam coal-fired power plant facility, located near Estevan, Saskatchewan, in the central plains of Canada. (Fig. 1). As of early 2024, more than 600 ktonnes of CO_2 have been stored permanently in the geological subsurface at Aquistore. The site comprises two wells, approximately 3400 meters deep, spaced 151 meters apart. One well functions as the injection well, while the other well serves as a monitoring well. CO_2 injection occurs via four perforated well sections, located at the most porous reservoir intervals with a total perforated section length of 150 m (Worth et al., 2014, Movahedzadeh et al., 2021). The observation well is not perforated to the reservoir but is equipped with the port of a fluid sampling system on the outside of the casing. Both wells are heavily equipped and are monitored using fibre optic technology and casing-conveyed pressure and temperature monitoring systems. Additional surface monitoring equipment include a comprehensive array of more than 630 permanently installed geophones, 6 broadband seismometers, a network of surface water wells and soil gas sampling stations, and tiltmeters and Interferometric Synthetic Aperture Radar (InSAR) reflectors (Worth et al., 2014).

In this study, our objective is to apply our recently developed IPSM workflow by simulating the extraction of geothermal energy through CO_2 circulation within the field-data-constrained reservoir model of the Aquistore CCS site. (Fig. 3). The reservoir model, incorporating the structural and heterogeneous variations encountered in nature, is employed to assess the effects of different fluids on geothermal energy extraction. The reservoir model represents the on-site situation as of April 15th, 2020. Fluid circulation is modelled via a 151 m spaced well doublet, mirroring the existing infrastructure at Aquistore (e.g. Rangriz Shokri & Chalaturnyk, 2021). More details on the history-matching process of the Aquistore model are provided in Sec. 2.2.

This approach aims at advancing our understanding of the dynamic interplay among fluid composition, reservoir conditions, and massflow rates. The goal is to identify efficient and sustainable geothermal energy extraction practices, while testing our developed IPSM workflow.

2. METHODOLOGY

To explore the research questions outlined above, we employ numerical reservoir simulation software, provided by the Computer Modelling Group Ltd. Our methodology revolves around the implementation of an integrated reservoir and production system modelling (IPSM) workflow. This approach enables a comprehensive investigation of the dynamic interactions among the reservoir, wellbore, and surface facilities, including re-injection processes.

2.1 Integrated Surface Wellbore Reservoir Modelling (IPSM) Workflow

In this work, a thermal multiphase, multicomponent simulator, GEM, was used to model the transient fluid flow in the subsurface formation. The Peng-Robinson equation of state (Peng & Robinson, 1976) was deployed to model the partitioning of the CO_2 and the brine components into different phases. The solubility of CO_2 in brine was modelled using Harvey's correlation for pure water, applying a correction for salinity (Harvey, 1996). The brine density was calculated by the Rowe and Chow brine density correlation (Rowe & Chou, 1970), while brine viscosity was determined following the method outlined by Kestin et al., 1981. The analytical infinite aquifer model, as proposed by Peck et al., 2014, was adopted, with salinity ranging between 271'000–336'000 ppm. The model was initialized with a pressure of 34,129.05 kPa and a temperature of 112.8°C at a depth of 3,173 m.

The thermal transient reservoir model was then coupled to a steady-state wellbore/facility simulator, CoFlow, to integrate the reservoir, wellbore, and facility components of the CPG cycle. The Gray correlation (Gray, 1978) was used to estimate the pressure drop along the wellbore for both the pure CO_2 case and the CO_2/water cases. The pure water case used the Beggs, Brill, Palmer, and Payne pressure drop correlation (Payne et al., 1979). These correlations are suitable for two-phase fluids and account for hydrostatic, friction, and acceleration components to compute the pressure changes along the pipes. The phase slippage and the flow pattern effects are also considered in these flow correlations. The heat transfer model predicts the pipe temperature profile as a function of the ambient temperature, inlet temperature, flow conditions, and an overall heat transfer coefficient. The overall heat transfer coefficient was calculated based on the tubing geometry and thermal conductivity of the material properties of the well.

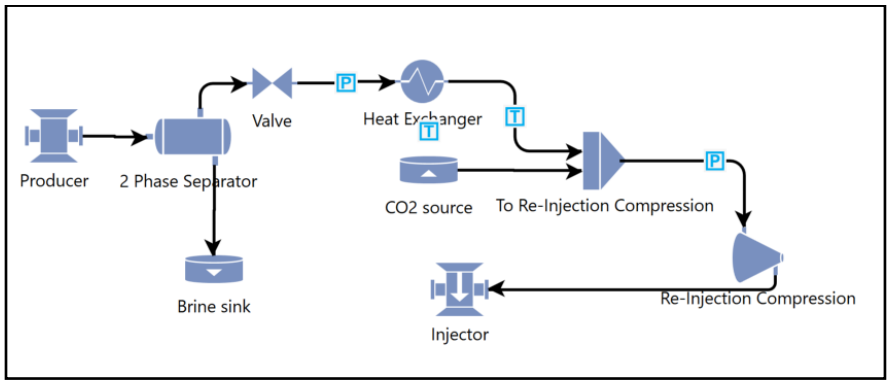

Figure 2: Visual representation of the surface facility model in the IPSM workflow. The depicted P and T letters signify pressure and temperature constraints, respectively. The model, starting at the producer wellhead, illustrates the transmission of production data, phase separation of CO_2 and water, and subsequent processes, providing an overview of the geothermal energy extraction and CO_2 reinjection cycle.

The surface facility model was included to simulate a conceptual and simplified geothermal power plant, serving as a vital element in the geothermal energy extraction cycle. Figure 3 provides a visual overview of the surface facility model. Initiating at the producer wellhead, production data, including pressure, temperature, and composition, is transmitted from the wellbore model at each timestep. The production stream undergoes a phase separation into its components – gaseous-like, supercritical CO_2, and liquid water. All produced water is assigned to a sink, while the produced CO_2 is depressurised to 6 MPa and cooled to a temperature of 22°C, representing geothermal energy extraction in a turbine and subsequent cooling and condensation into a subcooled liquid. These values were chosen based on prior studies, such as Adams et al., 2015. Idealized equipment settings are assumed to facilitate the conceptual understanding. The absence of considering pressure and temperature losses in the land-surface piping and in the other equipment is acknowledged, with future studies aiming to refine the model in this regard. After condensation, the produced CO_2 is merged with additional CO_2 coming from an external source. The combined fluid stream is isentropically compressed to the required injection pressure and delivered to the injector wellhead, where the injection data is then transferred to the wellbore model of the injection well. Flow in the entire system is governed by minimum and maximum bottomhole wellbore pressure constraints for the injector and producer, respectively. This approach enables the determination of theoretical maximum flow rates, providing insights into the capabilities of the existing infrastructure.

The thermal power generated, P_{th}, through the extraction of geothermal energy in the conceptual power plant (valve and heat exchanger in Fig. 2) as well as the thermal power required, P_{th}, for the isentropic recompression of the produced CO_2, were approximated using the formula: $P_{th} = \dot{m} * c_p * \Delta T$. Here, $\dot{m}$ represents the CO_2 mass flow rate [kg/sec], c_p is the isobaric specific heat capacity of CO_2 [0.849 kJ/(kg°C)], and ΔT stands for the temperature difference across the conceptual power inlet and outlet, respectively.

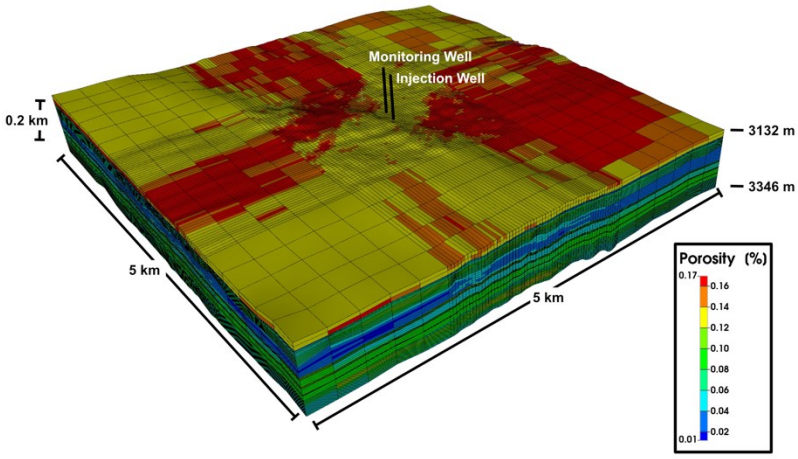

Figure 3: Three-dimensional view of the geological model, featuring superimposed dimensions, depth information, and the spatial distribution of porosity within the model.

2.2 Description of the HM Reservoir Model

The geological model was constructed across a 5 km x 5 km region, extending vertically from the Winnipeg Icebox to the Precambrian erosional surface. Utilising Petrel software, we incorporated geological and geophysical data, including well paths, logs, cores, and the interpreted seismic horizons. The porosity distribution was constrained to P-wave acoustic impedance, obtained from amplitude-variation-with-offset (AVO) inversion volumes. Porosity-permeability cross plots per facies were used as a secondary variable to populate the permeability in the model. The dynamic model was built and history-matched using the CMG compositional simulator (GEM) to match the CO_2 injection history of the Aquistore injection well in the target saline formations of the Black Island and lower Deadwood formation. Three sets of drainage relative permeabilities for different rock types (Bennion & Bachu, 2005; Kurz et al., 2014; Schlumberger, 2013).A summary of the parameters used to construct the geological model and to set up the flow simulation is shown in Table 2. The dynamic reservoir model was calibrated to the CO_2 injection history (injection rate, downhole pressure, and temperature), and available periodic logging data (e.g. spinner surveys at the injection well, pulsed-neutron log at the observation well) up to April 1st, 2020. The CO_2 plume shape from the model was also history-matched to the latest 4D seismic survey (Rangriz Shokri & Chalaturnyk, 2021).

Table 2: Overview of key flow simulation parameters, providing a summary of the crucial variables influencing the dynamic behaviour of the system.

Parameters	Values
Initial reservoir pressure, kPa	34129.05 at 3173 m MD
Pressure gradient, kPa/m	10.7
Initial reservoir temperature, ˚C	112.8 at 3173 m MD
Initial water saturation, fraction	1
Brine salinity, ppm	300’000
Porosity range, fraction	0.002-0.105
Permeability range, mD	0-55
Permeability anisotropy (k_v/k_h)	0.1
Reservoir boundary	Analytic infinite acting aquifer
Equation of State	Peng-Robinson
Default run type	Non-isothermal

3. RESULTS

This study seeks to show that the developed IPSM model is capable of simulating fluid circulation, heat extraction and fluid re-injection within a single simulated run, employing a field-data-informed reservoir model of the Aquistore site. The production and injection data of the tested scenario are shown in Figure 4. Injection and production massflow rates are presented in kg/sec. In the diagram, the solid lines represent the total (CO_2 + water) produced massflow rates, while the dotted lines indicate the injected CO_2 massflow rate.

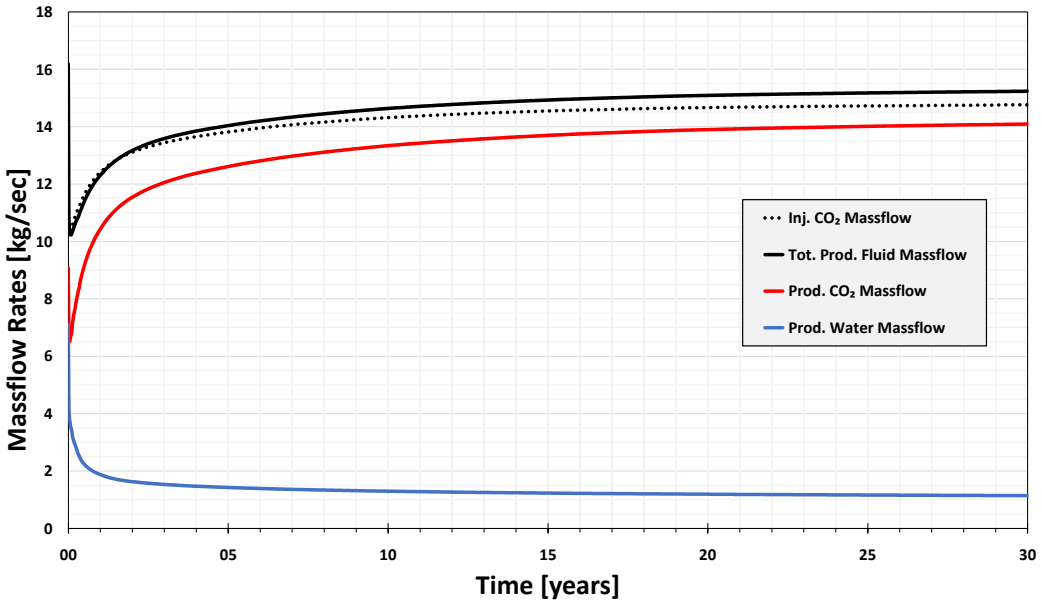

Figure 4: This diagram shows the massflow rates for the injection and production well as solid and dotted lines, respectively. Black indicates the total (CO_2 + water) massflow rate, blue the water massflow rate and red the CO_2 massflow rate.

Immediately after the start of fluid production, the total (CO_2 + water) produced massflow rate (solid black line) is sharply decreasing from around 16.2 kg/sec to a minimum of approximately 10.2 kg/sec. From this point onwards, the total produced fluid massflow rate increases continuously. For the first 1–2 years, after production start, the increase in the total produced fluid massflow rate is steep and flattens thereafter, stabilising at approximately 15 kg/sec. Almost identical observations can be made for the behaviour of the injection CO_2 massflow rate (black dotted lines), which, however, stabilises at around 14.7 kg/sec and thus slightly lower than the total produced fluid massflow rate.

Similarly, the massflow rate of the CO_2 component of the produced fluid (red line) drops from around 9 kg/sec after production start to a minimum value of around 7.5 kg/sec. Following the trend of the total produced fluid massflow rate (solid black line), the massflow rate of the CO_2 component also recovers and approaches a steady-state massflow rate of about 14 kg/sec. The produced water massflow rate in blue, drops sharply from more than 7.5 kg/sec, immediately after production start, to around 2 kg/sec at the end of year one. Around this time, the produced water massflow rate flattens out and reaches steady-state conditions at 1 kg/sec.

The bottom panel of Fig. 5 displays the temperature over the 30-year simulation period. Solid lines represent the producer, dotted lines the injector, and the green dashed line the heat exchanger outlet (see Fig. 3). Blue and red line represent bottom and tophole conditions, respectively. Over the simulation period, the bottom temperature in the production well (solid red line) decreases linearly from 113°C to 102°C. The tophole production well temperature (solid blue line) decreases from about 75°C to around 65°C during the first half year of the simulation. From this point onwards, the temperature decreases linearly to about 52°C. The dashed green line shows the constant heat exchanger outlet temperature of 22°C. The dotted blue line shows the constant tophole temperature of 40°C in the injection well. Depicted with the dotted red line, the bottomhole temperature in the injection well is constant at about 70°C.

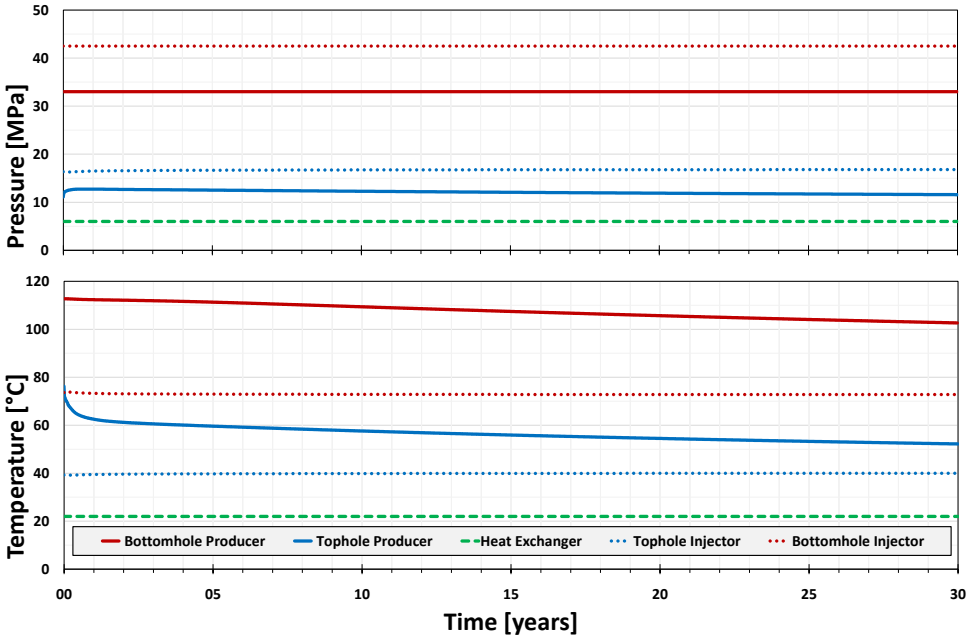

Figure 5: This diagram shows the pressure (top) and temperature (bottom) data of the production well (solid lines), the heat exchanger outlet (dashed green line), and the injection well (dotted lines) over time. The bottomhole and tophole well data are displayed in blue and red, respectively.

The pressure data at the top of Fig. 5 shows mostly constant values, except for the tophole production well pressure immediately after simulation start (solid blue line). The production well bottom-hole pressure, red solid line, is constant at 33 MPa. The tophole production well pressure increases from about 11.1 MPa to a constant value of around 12.7 MPa within the first few months after the simulation start. The power plant outlet pressure, dashed green line, is constant at 6 MPa. Injection well tophole (dotted blue line) and bottomhole (dotted red line) pressure values are constant at around 16.4 and 42.5 MPa, respectively.

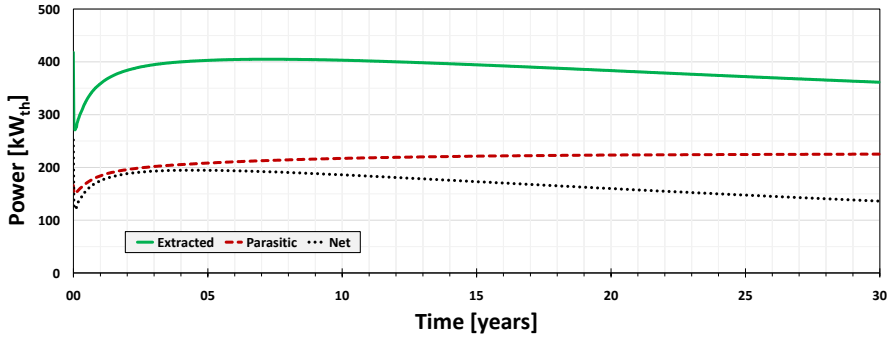

Figure 6: Plot showing the thermal power generated from CO_2 circulation in the simulated scenario. The solid green line represents the thermal power generated from the extracted geothermal energy from the reservoir, the dashed red line shows the parasitic thermal power necessary to isentropically compress the CO_2 for reinjection, and the black dotted line shows the net power available. (*It is important to note that the purpose of this study was not to optimize for power generation, but to show that the IPSM workflow is working.*)

Figure 6 provides an overview of the thermal power generated and required during the simulated CPG scenario in Kilowatts. The thermal power generated from the extracted geothermal energy is shown by the solid green line. Starting at 400 kW_{th} during simulation initiation, a minimum of approximately 270 kW_{th} is reached within the first month. Subsequently, there is a notable upswing, peaking at around 400 kW_{th}, which is followed by a gradual decline in thermal power in the years four to ten. After year ten, the generated thermal power gradually decreases to approximately 350 kW_{th}. The dashed red line represents the parasitic thermal power required for recompressing the produced CO_2 for reinjection. Initially, this parasitic thermal power is around 150 kW_{th}. Within the first fifteen years, the parasitic power requirement experiences an increase, reaching a consistent level of around 220–230 kW_{th}. The dotted black line shows the net power available for usage. Starting at a net available thermal power of around 250 kW_{th}, the net available power drops in alignment with the total power extracted (solid green line), reaching a minimum of 120 kW_{th}. Subsequently, there is a gradual increase in net thermal power peaking at 190 kW_{th} in years three to four. Following this maximum, the net available power decreases gradually to stabilise a final value of 120 kW_{th}.

4. DISCUSSION

The results demonstrate the capability of our newly developed Integrated Reservoir and Production System Modelling (IPSM) workflow to simulate CO_2-Plume Geothermal (CPG) operations for a field-data-informed, heterogeneous reservoir model of the Aquistore CCS site in Canada. Figure 4 indicates that fluid production from the existing non-perforated observation well would predominately result in CO_2 production, especially, once steady-state production rates are achieved after the first year. Under steady-state conditions, the massflow rate of produced water accounts for less than 10% of the total produced fluid massflow rate.

The sharp decrease of the production and injection CO_2 massflow rates immediately after simulation initiation is expected during the initiation phase of the CPG system (e.g. Ezekiel et al., 2022). During this phase the near wellbore region of the production well is drained of water/brine leading to temporarily increased massflow rates of produced water. Once conditions resembling steady-state are reached, the water cut drops significantly, causing the produced CO_2 massflow rate and, consequently, the total produced massflow rate to recover.

Stable, pseudo steady-state fluid production and CO_2 injection rates are achieved, with more CO_2 being injected than produced. Co-produced brine is removed in the conceptual surface facility. Pressure and temperature values align with expectations. The positive net power available indicates that the parasitic power required for isentropically recompressing the produced CO_2 for reinjection, along with the new CO_2 coming from the source, is less than the overall thermal power generated from the extracted geothermal energy. It is essential to emphasize that the presented scenario has not been optimized for power generation. Instead, our simulations serve as a case study to test the developed IPSM cycle for a field-data-informed, heterogeneous reservoir. For instance, the inner well radius of 0.0508 m used here is based on the currently existing wells at the Aquistore site. Commercial-scale CPG systems would employ significantly larger well radii (e.g. Adams et al., 2015), causing significantly lower pressure losses in the wellbores.

5. CONCLUSIONS

In essence, the simplified and conceptual surface facility model, which serves as the foundation of this study, plays a crucial role in establishing a robust Integrated Reservoir and Production System Modelling (IPSM) workflow for the comprehensive modelling of entire CO_2-Plume Geothermal (CPG) systems. The initial simplicity of the model enables a focused examination of distinct thermodynamic stages, leveraging valuable insights from previous research. Furthermore, this simplification serves as a starting point for future enhancements in model complexity.

In summary, our numerical study suggests that supercritical CO_2 can effectively serve as a geothermal energy extraction fluid at the Aquistore CCS site. The presented conceptual scenario, designed to test the functionality of the IPSM workflow, demonstrates that, based on the field-data-informed heterogeneous Aquistore reservoir model, predominantly CO_2 will be produced. This underscores that the higher mobility of CO_2 leads to a preferential inflow into the production well of CO_2, compared to in-situ water/brine. Moreover, the net thermal power available from this extraction of geothermal energy is positive, even in the thus far non-optimised production scenario.

6. OUTLOOK

The findings presented in this study illustrate the demand for an in-depth feasibility analysis to fully understand the implications of circulating CO_2 within a hypothetical CPG System at Aquistore. This analysis is not only crucial for the development and optimisation of an ideal well configuration and operational conditions but also for gaining a detailed understanding of the shape and behaviour of the thermal and pressure-depleted regions in the reservoir. Such a detailed assessment is indispensable for both research-oriented demonstrations and large-scale commercial implementations of CPG, accentuating the significance of various factors, such as well spacing and design as well as CPG operating conditions. The goal typically is to maximize CPG power output while keeping costs low, i.e. minimizing the Levelized Cost of Energy (LCOE) as well as maximizing the amount of sequestered CO_2.

Furthermore, a detailed examination of pressure and temperature depletion, resulting from the circulation of CO_2 at CCS sites, holds the potential to unveil a) additional CO_2 storage opportunities from re-pressurizing the decreased reservoir pressure with additional CO_2, or b) to advance the safety of CCS projects by reducing reservoir pore-fluid pressures so that caprock fracturing pressures are less likely reached. Such numerical explorations hold promise for enhancing the efficiency and safety of carbon capture, utilisation, and sequestration (CCUS) strategies.

6 ACKNOWLEDGEMENTS

We gratefully acknowledge support by the Werner Siemens Foundation (Werner Siemens-Stiftung) for its support of the Geothermal Energy and Geofluids (GEG.ethz.ch) group at ETH Zurich. We further gratefully acknowledge the Petroleum Technology Research Centre (PTRC), Regina, Saskatchewan, Canada, for discussions and advice regarding the Aquistore geologic CO_2 storage site, which they operate. This work has also been supported by the Energi Simulation Foundation. We acknowledge Schlumberger for providing the Petrel software package, and Computer Modelling Group LTD for providing the GEM and CoFlow Software package and for its support throughout the simulation phase of this study.

REFERENCES

Adams, B. M., Kuehn, T. H., Bielicki, J. M., Randolph, J. B., & Saar, M. O. (2015). A comparison of electric power output of CO_2 Plume Geothermal (CPG) and brine geothermal systems for varying reservoir conditions. *Applied Energy*, *140*, 365–377. https://doi.org/10.1016/j.apenergy.2014.11.043

Bell, I. H., Wronski, J., Quoilin, S., & Lemort, V. (2014). Pure and Pseudo-pure Fluid Thermophysical Property Evaluation and the Open-Source Thermophysical Property Library CoolProp. *Industrial & Engineering Chemistry Research*, *53*(6), 2498–2508. https://doi.org/10.1021/ie4033999

Bennion, B., & Bachu, S. (2005, October). *Relative Permeability Characteristics for Supercritical* CO_2 *Displacing Water in a Variety of Potential Sequestration Zones in the Western Canada Sedimentary Basin*.

Catuneanu, O. (2022). *Principles of Sequence Stratigraphy*. Elsevier. https://doi.org/10.1016/C2009-0-19362-5

Ezekiel, J., Adams, B. M., Saar, M. O., & Ebigbo, A. (2022). Numerical analysis and optimization of the performance of CO_2-Plume Geothermal (CPG) production wells and implications for electric power generation. *Geothermics*, *98*. https://doi.org/10.1016/j.geothermics.2021.102270

Gray, H. E. (1978). Vertical Flow Correlation in Gas Wells. In *User's Manual for API 14B Surface Controlled Subsurface Safety Valve Sizing Computer Program*. American Petroleum Institute,.

Guyant, E., Han, W. S., Kim, K. Y., Park, M. H., & Kim, B. Y. (2015). Salt precipitation and CO_2/brine flow distribution under different injection well completions. *International Journal of Greenhouse Gas Control*, *37*, 299–310. https://doi.org/10.1016/j.ijggc.2015.03.020

Harvey, A. H. (1996). Semiempirical correlation for Henry's constants over large temperature ranges. *AIChE Journal*, *42*(5), 1491–1494. https://doi.org/10.1002/aic.690420531

IEA. (2023). *World Energy Outlook 2023*. https://www.iea.org/reports/world-energy-outlook-2023

IPCC. (2023). *Climate Change 2023: Synthesis Report. Contribution of Working Groups I, II and III to the Sixth Assessment Report of the Intergovernmental Panel on Climate Change* (P. Arias, M. Bustamante, I. Elgizouli, G. Flato, M. Howden, C. Méndez-Vallejo, J. J. Pereira, R. Pichs-Madruga, S. K. Rose, Y. Saheb, R. Sánchez Rodríguez, D. Ürge-Vorsatz, C. Xiao, N. Yassaa, J. Romero, J. Kim, E. F. Haites, Y. Jung, R. Stavins, Leprince-Ri, Eds.). https://doi.org/10.59327/IPCC/AR6-9789291691647

Kestin, J., Khalifa, H. E., & Correia, R. J. (1981). Tables of the dynamic and kinematic viscosity of aqueous NaCl solutions in the temperature range 20–150 °C and the pressure range 0.1–35 MPa. *Journal of Physical and Chemical Reference Data*, *10*(1), 71–88. https://doi.org/10.1063/1.555641

Kreis, L. K., Haidl, F. M., Nimegeers, A. R., Ashton, K. E., Maxeiner, R. O., & Coolican, J. (2004). *Lower Paleozoic Map Series Saskatchewan Saskatchewan*.

Kurz, M., Heebink, L., Smith, S., & Zacher, E. (2014). *Petrophysical Evaluation of Core from the Aquistore* CO_2 *Injection Site. Plains* CO_2 *Reduction (PCOR) Partnership value-added report for U.S. Department of Energy National Energy Technology Laboratory Cooperative Agreement No. DE-FC26-05NT42592, EERC Publication 2014-EERC-07-16,*.

Movahedzadeh, Z., Shokri, A. R., Chalaturnyk, R., Nickel, E., & Sacuta, N. (2021). Measurement, monitoring, verification and modelling at the Aquistore CO_2 storage site. *First Break*, *39*(2), 69–75. https://doi.org/10.3997/1365-2397.fb2021013

Payne, G. A., Palmer, C. M., Brill, J. P., & Beggs, H. D. (1979). Evaluation of Inclined-Pipe, Two-Phase Liquid Holdup and Pressure-Loss Correlation Using Experimental Data (includes associated paper 8782). *Journal of Petroleum Technology*, *31*(09), 1198–1208. https://doi.org/10.2118/6874-PA

Peck, W. D., Bailey, T. P., Liu, G., Klenner, R. C. L., Gorecki, C. D., Ayash, S. C., Steadman, E. N., & Harju, J. A. (2014). Model development of the Aquistore CO_2 storage project. *Energy Procedia*, *63*, 3723–3734. https://doi.org/10.1016/j.egypro.2014.11.401

Peng, D.-Y., & Robinson, D. B. (1976). A New Two-Constant Equation of State. *Industrial & Engineering Chemistry Fundamentals*, *15*(1), 59–64. https://doi.org/10.1021/i160057a011

PTRC. (2015). *Aquistore Project summary report*. http://www.ptrc.ca

Randolph, J. B., & Saar, M. O. (2011). Combining geothermal energy capture with geologic carbon dioxide sequestration. *Geophysical Research Letters*, *38*(10). https://doi.org/10.1029/2011GL047265

Rangriz Shokri, A., & Chalaturnyk, R. (2021). *Feasibility Study for Proposed* CO_2 *Circulation Test at the Aquistore Injection Site, Saskatchewan*. www.bfe.admin.ch

Rowe, A. M., & Chou, J. C. S. (1970). Pressure-volume-temperature-concentration relation of aqueous sodium chloride solutions. *Journal of Chemical & Engineering Data*, *15*(1), 61–66. https://doi.org/10.1021/je60044a016

Schlumberger Reservoir Laboratories. (2013). *Relative Permeability by Unsteady-State Method: Prepared for Petroleum Technology Reserach Centre, Well: 5-6-2-8, Regina Saskatchewan*.

White, D. J., Hawkes, C. D., & Rostron, B. J. (2016). Geological characterization of the Aquistore CO_2 storage site from 3D seismic data. *International Journal of Greenhouse Gas Control*, *54*, 330–344. https://doi.org/10.1016/j.ijggc.2016.10.001

Worth, K., White, D., Chalaturnyk, R., Sorensen, J., Hawkes, C., Rostron, B., Johnson, J., & Young, A. (2014). Aquistore project measurement, monitoring, and verification: From concept to CO_2 injection. *Energy Procedia*, *63*, 3202–3208. https://doi.org/10.1016/j.egypro.2014.11.345

Worth, K., White, D., Chalaturnyk, R., Sorensen, J., Hawkes, C., Rostron, B., Risk, D., Young, A., & Sacuta, N. (2017). Aquistore: Year One - Injection, Data, Results. *Energy Procedia*, *114*, 5624–5635. https://doi.org/10.1016/j.egypro.2017.03.1701